

## Original article

# Quantitative characterization of micropore structure for organic-rich Lower Silurian shale in the Upper Yangtze Platform, South China: Implications for shale gas adsorption capacity

Lei Chen<sup>1,2,3</sup>, Zhenxue Jiang<sup>1,2\*</sup>, Keyu Liu<sup>4,5</sup>, Fenglin Gao<sup>1,2</sup>

<sup>1</sup>State Key Laboratory of Petroleum Resources and Prospecting, China University of Petroleum, Beijing 102249, P. R. China

<sup>2</sup>Unconventional Natural Gas Institute, China University of Petroleum, Beijing 102249, P. R. China

<sup>3</sup>Unconventional Oil & Gas Cooperative Innovation Center, China University of Petroleum, Beijing 102249, P. R. China

<sup>4</sup>CSIRO Earth Science and Resource Engineering, Bentley WA 6102, Australia

<sup>5</sup>School of Geosciences, China University of Petroleum, Qingdao 266580, P. R. China

(Received August 10, 2017; revised August 28, 2017; accepted August 29, 2017; published September 25, 2017)

**Abstract:** The pores in shales are mainly of nanometer-scale, and their pore size distribution is very important for shale gas storage and adsorption capacity, especially micropores having widths less than 2 nm, which contribute to the main occurrence space for gas adsorption. This study is focused on the organic-rich Lower Silurian black shale from four wells in the Upper Yangtze Platform, and their total organic carbon (TOC), mineralogical composition and micropore characterization were investigated. Low pressure CO<sub>2</sub> adsorption measurement was conducted at 273.15 K in the relative pressure range of 0.0001-0.03, and the micropore structure was characterized by Dubinin-Radushkevich equation and density functional theory method and then the relationship between micropore structure and shale gas adsorption capacity was discussed. The results indicated that (1) The Lower Silurian shale have high TOC content in the range of 0.92%-4.96%, high quartz content in the range of 30.6%-69.5%, and high clays content in the range of 24.1%-51.2%. The TOC content shows a strong positive relationship with the quartz content which suggests that the quartz is mainly biogenic in origin. (2) The micropore volume varies from 0.12 to 0.44 cm<sup>3</sup>/100g and micropore surface area varies from 4.97 to 17.94 m<sup>2</sup>/g. Both of them increase with increasing TOC content, indicating TOC is the key factor to control the micropore structure of the Lower Silurian shale. (3) Low pressure CO<sub>2</sub> adsorption measurement provides the most suitable detection range (0.3-1.5 nm) and has high reliability and accuracy for micropore structure characterization. (4) The TOC content is the key factor to control gas adsorption capacity of the Lower Silurian shale in the Upper Yangtze Platform.

**Keywords:** Shale gas, micropore structure, lower silurian shale, Upper Yangtze Platform, adsorption capacity.

**Citation:** Chen, L., Jiang, Z., Liu, K., et al. Quantitative characterization of micropore structure for organic-rich Lower Silurian shale in the Upper Yangtze Platform, South China: Implications for shale gas adsorption capacity. *Adv. Geo-Energy Res.* 2017, 1(2): 112-123, doi: 10.26804/ager.2017.02.07.

## 1. Introduction

Shale is a kind of dense rocks with extremely low porosity and permeability (Chen et al., 2011, 2014, 2016; Du et al., 2015; Wei et al., 2016a). However, natural gas can be stored as free gas or adsorbed gas in the nanoscale pores of shale reservoirs (Gasparik et al., 2014; Ji et al., 2015, 2016; Li et al., 2015a). The classification of the nanoscale pore size in the

shale mainly accords to the

International Union of Pure and Applied Chemistry (IUPAC) standard, namely the pore width less than 2 nm for micropore, pore width between 2 and 50 nm for mesopore, pore width greater than 50 nm for macropore (Sing, 1985). Pore structure characteristics contribute significantly to the gas storage and adsorption capacity of shales (Ross and Bustin, 2009; Slatt and O'Brien, 2011; Wei et al., 2014; Jing et al.,

\*Corresponding authors. Email: jzxuecup@126.com

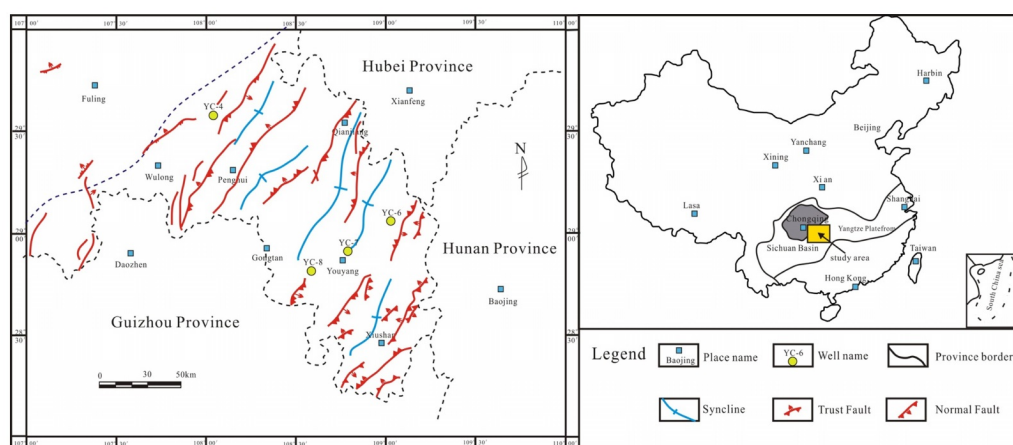


**Fig. 1.** Schematic map showing sample wells location (modified from Ji et al., 2015).

**Table 1.** Lithology (Black shale), depth, TOC and mineralogical composition for shale samples.

Sample ID	Well	Depth (m)	TOC (%)	Mineralogical composition relative percent (%)					CO <sub>2</sub> adsorption analysis	
				Quartz	Feldspar	Carbonates	Pyrite	Total clays	Micropore surface area (m <sup>2</sup> /g)	Micropore volume (cm <sup>3</sup> /100g)
S-1	YC4	675.3	2.07	30.6	6.5	10.0	1.7	51.2	12.05	0.28
S-2	YC4	756.4	4.96	69.5	2.8	0	3.6	24.1	17.07	0.42
S-3	YC4	758.5	4.60	66.2	4.2	0	2.0	27.6	17.94	0.44
S-4	YC6	751.6	0.92	34.0	15.3	0	4.2	46.5	4.97	0.12
S-5	YC6	769.7	1.71	40.4	11.2	7.1	3.1	38.2	8.27	0.22
S-6	YC6	774.2	3.13	45.8	9.8	6.5	0	37.9	10.86	0.30
S-7	YC7	861.2	2.50	39.0	8.6	7.5	0	44.9	11.43	0.29
S-8	YC8	900.3	3.35	46.1	5.0	7.5	4.8	36.6	13.25	0.35

2016; Li et al., 2016). Although mesopores and macropores might be present, micropores dominate in gas shale systems (Bu et al., 2015; Yang et al., 2016a). Therefore, it is very important to study the micropore structure of shales in order to evaluate the gas-bearing property and guide the exploration and development of shale gas.

The pore structure characterization methods can be divided into two categories: (1) Direct method. To directly observe and obtain image by means of optical microscope, transmission electron microscope (TEM), scanning electron microscope (SEM), and other micro zone observation technologies in order to get the size, shape and distribution of pores and other qualitative informations in shales (Chalmers et al., 2012; Curtis et al., 2012; Loucks et al., 2012; Gu et al., 2015; Klaver et al., 2015, 2016; Li et al., 2015b; Tang et al., 2016; Zhou et al., 2016); (2) Indirect method. Mainly by means of probe gas adsorption techniques to quantitatively characterize the pore size and pore structure, including neutron scattering, high pressure mercury intrusion, low pressure gas adsorption and so on (Mastalerz et al., 2012, 2013; Clarkson et al., 2013; Cao et al., 2015; Hu et al., 2015). Due to the complexity of sample preparation and limited observation area, microscopic observation method has a certain limit and generally only be used for qualitative analysis (Jiao et al., 2014; Yang et

al., 2016a, 2016b; Zeng et al., 2016). High pressure mercury intrusion method provides both porosity value and the distribution characteristics of pores (Clarkson et al., 2013), however, pressure resistance of shale is much worse than sandstone and the pores in shale mainly consist of nanoscale pore, it will lead to some secondary macropores (Giesche, 2006). Neutron scattering is not ready yet for general use due to its high costs. Compared with the above methods, low pressure gas adsorption technology can avoid man-made macropore, and can also provide pore parameters such as pore distribution and specific surface area, therefore it has been widely used in the shale nanopore size analysis (Tian et al., 2013, 2015; Cao et al., 2015; Pan et al., 2015; Zhang et al., 2015; Yang et al., 2016a, 2016b, 2016c; Zeng et al., 2016).

Since shale gas can be stored in the form of adsorbed gas (Zhang et al., 2012; Rexer et al., 2013; Wu et al., 2015) and the adsorption behavior of gas in micropores is significantly different from that in mesopores or macropores (Tian et al., 2015; Yang et al., 2016c), it is necessary to quantitatively evaluate the micropores in shales. This research focuses on the micropore structure characteristics of the Lower Silurian shale in the Upper Yangtze Platform, South China. In this study, low pressure CO<sub>2</sub> adsorption measurement for shale samples was conducted to (1) characterize the micropore structure (includ-

ing micropore surface area, micropore volume, and micropore size distribution) of the studied shale; and (2) discuss the micropore structure in relation to gas adsorption capacity of the studied shale. Our studies are of great significance for the assessment and exploitation of natural gas in the shale reservoirs.

## 2. Samples and methods

### 2.1 Geological setting and samples

The Yangtze Platform is one of the three oldest platforms in South China and is split into three parts that are consistent with the upper, middle, and lower. The Upper Yangtze Platform is located in the western part of the Yangtze Platform (Fig. 1) and experienced uplift and subsidence during the Palaeozoic. Marine sediments covered the platform after the early Palaeozoic, and these sedimentary rocks include very thick shale deposits. There were three major shale-forming periods during the Palaeozoic (Cai et al., 2016). Shale developed well on the deepwater shelf and there was a carbonate platform in the shallow waters and in the horizons of shale in the Upper Yangtze Platform; these are found mainly in the Lower Cambrian, Lower Silurian, and Permian (Fig. 2). The Lower Silurian shale, widely developed in the Upper Yangtze Platform, has recently been selected as the main target for shale gas exploration and development (Chen et al., 2011, 2014; Tan et al., 2014; Ji et al., 2015, 2016; Jiang et al., 2016; Liu et al., 2016; Tang et al., 2016; Yang et al., 2016a, 2016b, 2016c). The Silurian shales occur in some strongly uplifted areas as outcrops, which indicates that the shales have experienced a complicated tectonic evolution, then influencing the gas content (Hao et al., 2013).

Black shales are present in the Lower Silurian Longmaxi formation in the Upper Yangtze Platform with current burial depth of 1000-5000 m (Pan et al., 2016). The thickness generally ranges from 50 to 100 m with an EqRo of 2.5%-3.0%, generating mainly dry gas and secondary gas (Tan et al., 2014; Pan et al., 2016).

In the present study, eight shale samples from the Lower Silurian Longmaxi shale were collected from four wells in the Upper Yangtze Platform, South China. The sampling well locations are shown in Fig. 1. All the shale samples were collected from fresh core materials, with the weight up to 120-200 g. Each of them was then crushed to 60 mesh particle size below and got sufficiently mixed. Sample information such as ID, TOC and other geological parameters are listed in Table 1.

### 2.2 TOC and X-ray diffraction analysis

TOC content analysis was performed for shale samples using a Leco CS-230 analyzer at State Key Laboratory of Petroleum Resources and Prospecting in China University of Petroleum (Beijing). To remove carbonates, about 100 mg was placed in a crucible with 5% HCl at the temperature of 80 °C.

Quantitative X-ray diffraction (XRD) analysis of randomly oriented powders was used for the mineralogy of the shale

sample study at Experimental Research Center of East China Branch, SINOPEC. The measurements were performed on Ultima IV diffractometer using Cu K $\alpha$ -radiation ( $\lambda = 0.15418$  nm) produced at a voltage of 40 kV and a current of 40 mA. A scan rate of 4°(2 $\theta$ )/min was used in the range of 5°-45° for the recording of the XRD traces. In the beginning, the bulk mineral composition of the powder sample was determined, but at this stage only the total clay content was included. Then moving to the next stage, the individual mineral content of clay fractions, which was separated from the rock powder sample was determined. Please be noted that in this experiment both the bulk and individual contents were measured under exactly the same conditions.

### 2.3 Low pressure CO<sub>2</sub> adsorption measurement

As mentioned previously, low pressure gas adsorption measurements have been widely used in the shale nanopore size analysis. However, low pressure N<sub>2</sub> adsorption measurement only can be used to characterize pore size distribution from mesopores to macropores in shale, and the precision is not high for micropore (Wei et al., 2016a). Low pressure CO<sub>2</sub> adsorption measurement is more suitable for characterizing micropores in shale because of its smaller molecular detection diameter and lower experimental relative pressure (Yang et al., 2016c).

Low pressure CO<sub>2</sub> adsorption analysis was performed using a Micromeritics ® Tristar II 3020 surface area analyzer at State Key Laboratory of Heavy Oil Processing in China University of Petroleum, Beijing. Shale sample aliquots weighing 1 to 2 g were analyzed with CO<sub>2</sub> to obtain information about micropore structure. Samples were automatically degassed at about 110°C under vacuum for about 14 h to remove adsorbed moisture and volatile matter before analyzing with CO<sub>2</sub>. The sample was maintained at the temperature of 273.15 K to measure CO<sub>2</sub> adsorption. The equilibrium interval (time over which the pressure must remain stable within a very small range) was set at 45 s, and the relative pressure (P/P<sub>0</sub>) ranges from 0.0001 to 0.03. Based on multiple adsorption theories, the instrument's computer software automatically generates adsorption isotherms and calculates pore distributions (Mastalerz et al., 2012, 2013).

### 2.4 Dubinin-Radushkevich equation

Because of a large amount of developed micropores in the shales, the adsorption behavior of gas in micropores can be significantly different from that in mesopores or macropores (Mosher et al., 2013). Instead of the surface adsorption mechanism described by the Brunauer-Emmett-Teller (BET) theory, the adsorption behavior in micropores is the filling of gas. The Dubinin-Radushkevich (DR) equation can be used to describe the gas filling the micropores. The DR equation has the following form:

$$\log(V_{ads}) = \log(V_{mic}) - 2.303 \left( \frac{RT}{\beta E_0} \right)^2 \log^2 \left( \frac{P}{P_0} \right) \quad (1)$$

where  $V_{ads}$  is the adsorbed volume (cm<sup>3</sup>/g),  $V_{mic}$  is the

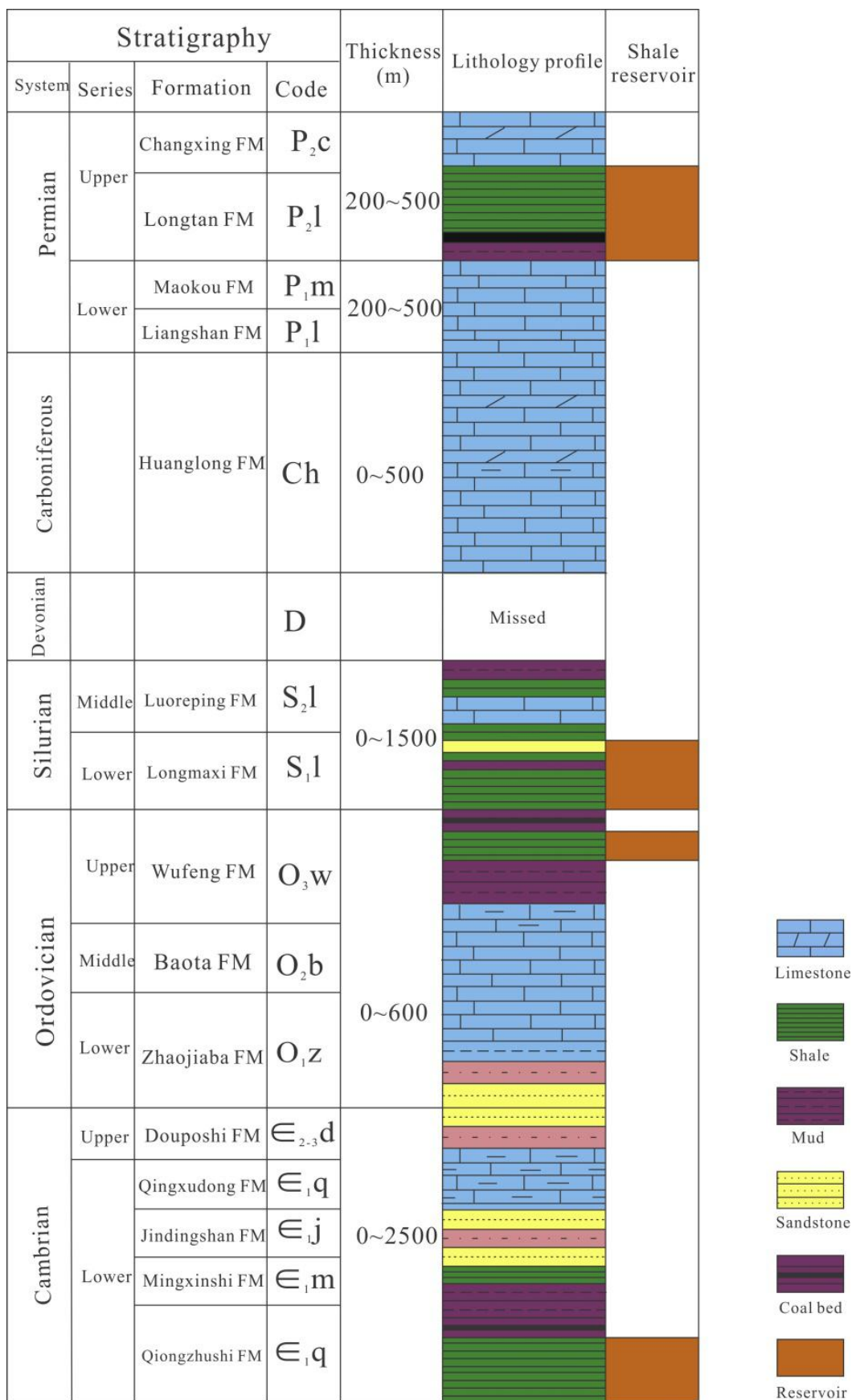
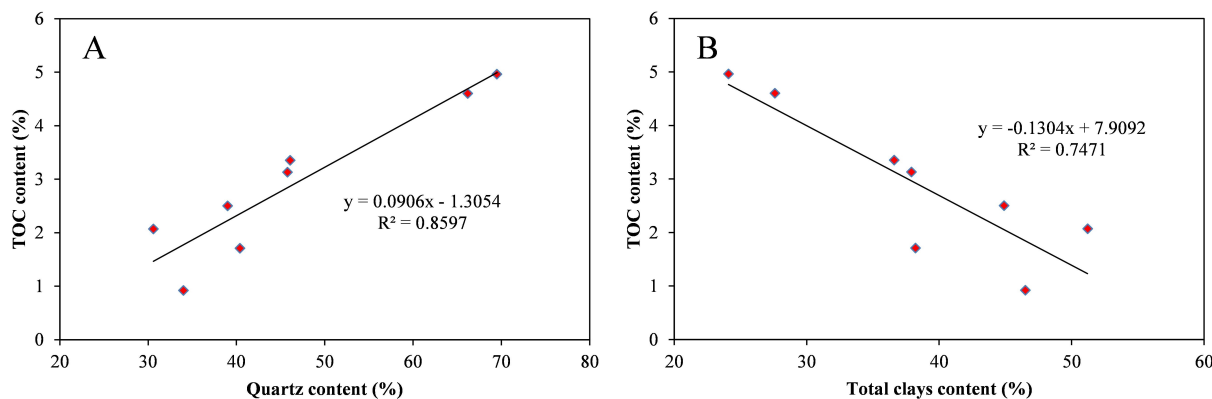


Fig. 2. Stratigraphical column showing the black shales in the Upper Yangtze Platform (modified from Cai et al., 2016).



**Fig. 3.** Plots showing the relationships of TOC content with quartz content (A) and total clays content (B) of the shale samples.

micropore volume ( $\text{cm}^3/\text{g}$ ),  $T$  is the Kelvins temperature (K),  $R$  is the gas constant ( $0.008314 \text{ kJ/mol/K}$ ),  $\beta$  is the affinity coefficient,  $E_0$  is the characteristic energy ( $\text{kJ/mol}$ ) dependent on the pore structure,  $P$  is equilibrium pressure (MPa) and  $P_0$  is saturation vapor pressure (MPa).

Then, the mean pore width could be estimated by the following equation when the characteristic energy is between 20 and 42  $\text{kJ/mol}$ :

$$L = \frac{10.8}{E_0 - 11.4} \quad (2)$$

where  $L$  is the mean pore width (nm), and  $E_0$  is the characteristic energy ( $\text{kJ/mol}$ ). This range of energies corresponds to pore sizes between 0.35 and 1.3 nm for which the validity of this equation has been tested (Stoeckli and Ballerini, 1991). The Dubinin equation (Dubinin, 1985) has been used for lower values of  $E_0$  (i.e., higher pore size):

$$L = \frac{24}{E_0} \quad (3)$$

Assuming that the pores in shale are mainly composed of spherical pores, then the following equation was used to calculate the micropore surface area ( $S_{mic}$ ):

$$S_{mic} = \frac{6V_{mic}}{L} \quad (4)$$

### 2.5 Density functional theory (DFT) method

As method for micropore size distribution analysis of organic-rich shale, DFT method is now available for  $\text{CO}_2$  adsorption system (Tian et al., 2013, 2015; Wei et al., 2016b; Yang et al., 2016a, 2016b). Pores within the range of 0.3-1.5 nm can be explored with  $\text{CO}_2$  at 273.15 K in the relative pressure range of 0.0001-0.03 using DFT method. Thus, low pressure  $\text{CO}_2$  adsorption could be used to characterize micropore structure of organic-rich shale and has high reliability and accuracy.

## 3. Results and discussion

### 3.1 TOC and mineralogical composition

The TOC contents of shale samples presented in Table 1

range from 0.92% to 4.96% with an average of 2.91%. Based on the measured TOC contents, most of the shale samples are categorized as organic-rich shales, which agree well with previous results from the Lower Silurian shales in this region (Ji et al., 2015, 2016; Cai et al., 2016).

The mineralogical composition of shale samples obtained from XRD analysis is tabulated in Table 1. The shale samples contained abundant quartz and clay minerals. There is a large variation in the quartz content in these shale samples. The quartz content ranged from 30.6% to 69.5% with an average of 46.5%. In addition to quartz, clay mineral is also the major mineral in the shale samples with a percentage of 24.1%-51.2%. The clay mineral composition generally reflects the diagenetic evolution and depositional environments and they are important to the study of methane sorption and gas content of the shale (Wang et al., 2013). Feldspar is in significant quantity in the shale samples with a range of 2.8%-15.3%. Other minerals, e.g., carbonates and pyrite, occurred occasionally with a percentage of 6.5%-10.0% and 1.7%-4.8%, respectively.

TOC values of eight shale samples show a strong positive correlation ( $R^2 = 0.8597$ ) with the quartz content (Fig. 3A), which is also observed in Devonian shale samples from the Horn River Basin, Canada (Chalmers et al., 2012; Dong et al., 2015). The positive relationship suggests that the quartz is mainly biogenic in origin, which has also been proved in the Lower Silurian shales in this region (Yang et al., 2016a, 2016c). A negative correlation between TOC and total clays content is observed for the studied samples ( $R^2 = 0.7471$ , Fig. 3B) and attributed this to decreasing total clays content with an increase of quartz content.

### 3.2 Isotherms of $\text{CO}_2$ adsorption

The adsorption isotherms of  $\text{CO}_2$  are shown in Fig. 4 and similar to Type I adsorption isotherm recommended by IUPAC, the existence of micropores is indicated. When the experimental relative pressure reaches the maximum value ( $P/P_0 = 0.03$ ), the adsorption amounts show a large difference, varying between 0.40 and 1.53  $\text{cm}^3/\text{g}$ . It is clear that there is a significantly positive correlation between the maximum adsorption amount and the TOC content.

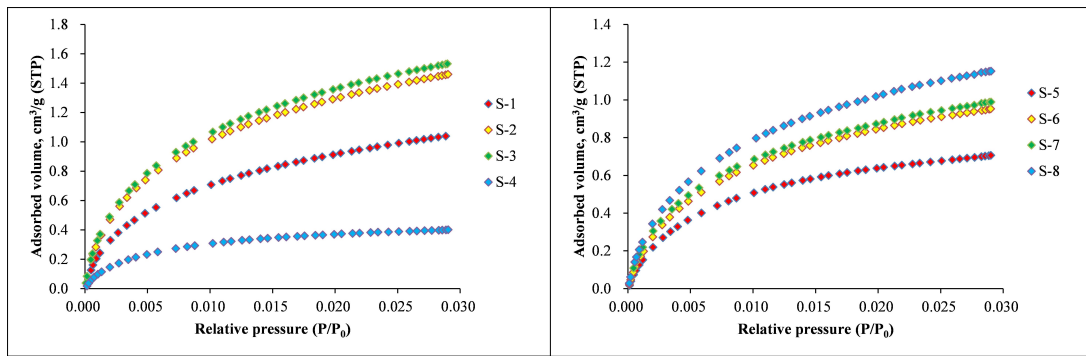


Fig. 4. CO<sub>2</sub> adsorption isotherms of the shale samples.

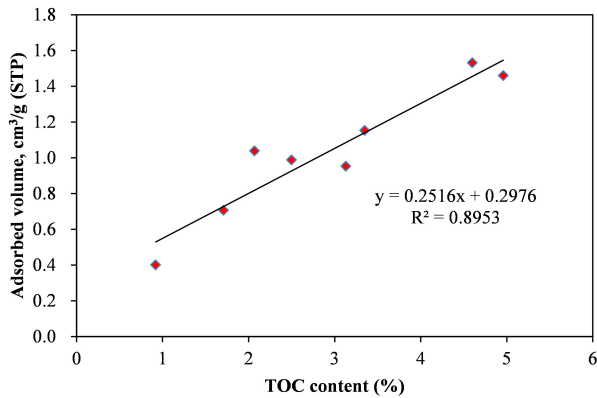


Fig. 5. Plot showing the relationship between the maximum CO<sub>2</sub> adsorption amount at  $P/P_0 = 0.03$  and TOC content of the shale samples.

orption amount and the TOC content (Fig. 5), indicating that the organic matters in the shales are important spaces for micropores development. In other words, the higher the organic matter content, the better the micropore development.

### 3.3 Micropore volume/surface area analysis

Table 1 shows the micropore volume/surface area that were determined from the CO<sub>2</sub> adsorption isotherms using the DR equation. Fig. 6 shows the micropore volume ( $V_{mic}$ ) for eight shale samples ranges from 0.12 to 0.44 cm<sup>3</sup>/100g, which has a strong positive correlation with the TOC content ( $R^2 = 0.9336$ ). Fig. 7 shows the micropore surface area ( $S_{mic}$ ) for eight shale samples ranges from 4.97 to 17.94 m<sup>2</sup>/g, which has also a strong positive correlation with the TOC content ( $R^2 = 0.8962$ ). These agree well with previous results from gas shales in North American basins (Chalmers and Bustin, 2008; Ross and Bustin, 2009) and Lower Silurian and Lower Cambrian shales in southwestern China (Tian et al., 2013, 2015). They both suggest that organic matters provide important spaces for micropores development in the Lower Silurian shale, which has also been reported in other shales (Milliken et al., 2013; Tian et al., 2013, 2015). In addition to organic matter abundance, organic matter maturity also plays an important role for micropore development, which has been

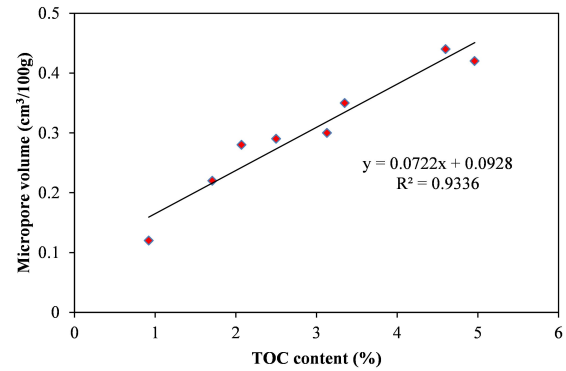


Fig. 6. Plot showing the relationship between micropore volume and TOC content of the shale samples.

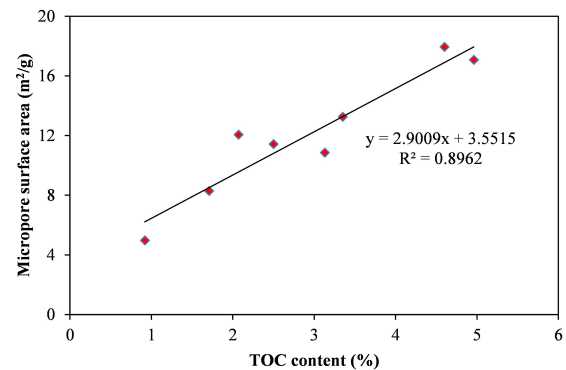


Fig. 7. Plot showing the relationship between micropore surface area and TOC content of the shale samples.

reported in other shale (Chen and Xiao, 2014). Especially when maturity value ( $R_o$ ) is greater than 2%, the increase of micropore volume and micropore surface area is very obvious and attributed this to increasing organic matter nanopore with increasing maturation (Mastalerz et al., 2013; Chen and Xiao, 2014; Romero-Sarmiento et al., 2014).

### 3.4 Pore size distributions ( $PSD_s$ )

A plot of  $dV/dD$  or  $dS/dD$  versus  $D$  (pore diameter) for CO<sub>2</sub> is commonly used to illustrate the micropore size

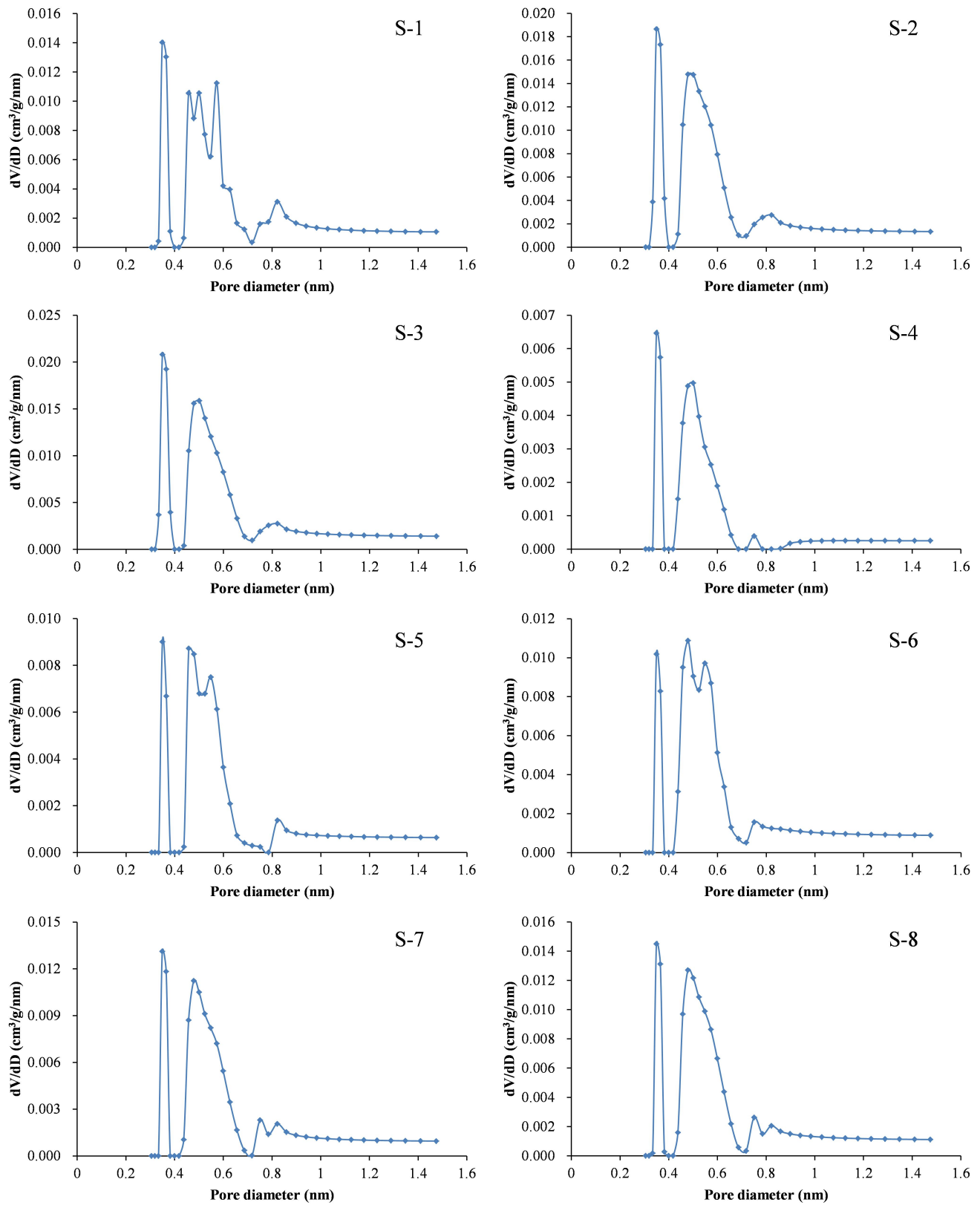


Fig. 8. Plots of dV/dD versus D for micropore size distribution of the shale samples.

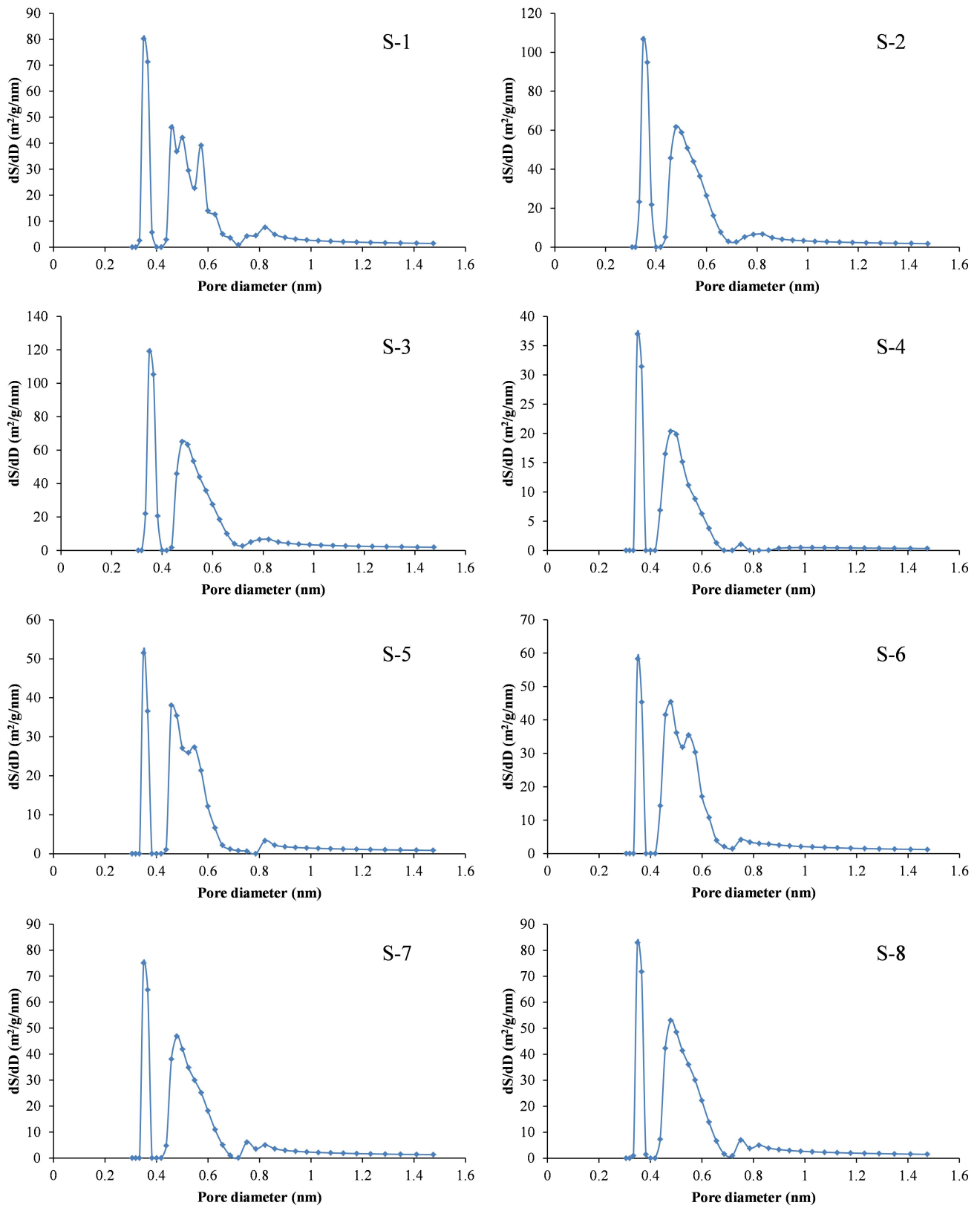


Fig. 9. Plots of  $dS/dD$  versus  $D$  for micropore size distribution of the shale samples.

distribution (Tian et al., 2013; Li et al., 2016), and is used to compare the relative micropore volumes or micropore surface areas between any pore size ranges, because the “visual area” under the curve of  $dV/dD$  or  $dS/dD$  is proportional to the real volume or surface area.

Micropore size analysis with the range of 0.3-1.5 nm can be explored based on  $\text{CO}_2$  adsorption isotherms using the DFT method. Figs. 8 and 9 show the micropore volume and micropore surface area distributions with pore diameter of the shale samples, respectively. The micropore size distribution curves vary from sample to sample (Figs. 8 and 9), as mentioned previously, the difference is mainly caused by different TOC contents of shale samples.

The results from our study show that the most suitable critical range of 0.3-1.5 nm can be analyzed with low pressure  $\text{CO}_2$  adsorption, which agree well with previous results from the Lower Silurian and Lower Cambrian shales in this region (Sun et al., 2016; Wei et al., 2016b; Yang et al., 2016c). More details will be discussed in a following study.

### 3.5 Shale gas adsorption capacity

Shale gas is stored in three different types of geological environment and they are (1) free gas in pores and fractures, (2) adsorbed gas in organic matters and clay minerals, (3) dissolved gas in residual oil and water (Zhang et al., 2012; Hao et al., 2013; Rexer et al., 2013; Ji et al., 2015; Wu et al., 2015; Chen et al., 2017a, 2017b). Free gas and adsorbed gas are predominant in high-maturity shales (Hao et al., 2013). Adsorbed gas is located mainly within micropores and at the surface of mesopores and macropores, while free gas is mainly stored in macropores and larger mesopores (Fig. 10; Pan et al., 2015). As previously discussed, it is clear that the organic matter mainly controls the micropore structure of the Lower Silurian shale, thus influencing gas adsorption capacity.

As discussed previously, it can be concluded that the shales with higher TOC content show better developed micropores. This indicates that, in general, smaller pores dominate the samples with elevated TOC content. Our study also shows that the samples with low TOC content (<2%) have micropore surface area <9  $\text{m}^2/\text{g}$ , indicating lower gas adsorption capacity. Samples with TOC content between 2% and 4% have micropore surface area of 10-14  $\text{m}^2/\text{g}$ , and the gas adsorption capacity increases with increasing TOC content. Samples with high TOC content (>4%) have micropore surface area of >17  $\text{m}^2/\text{g}$ , which implies higher gas adsorption capacity.

Such a pattern is quite analogous to previous studies (e.g., Ji et al., 2015; Wu et al., 2015) and is of great significance for understanding the changes in gas adsorption capacity of organic-rich shales.

## 4. Conclusions and suggestion

Low pressure  $\text{CO}_2$  adsorption measurement was used to characterize the micropore structure of organic-rich Lower Silurian shale in the Upper Yangtze Platform, South China. The following are the main conclusions from our study:

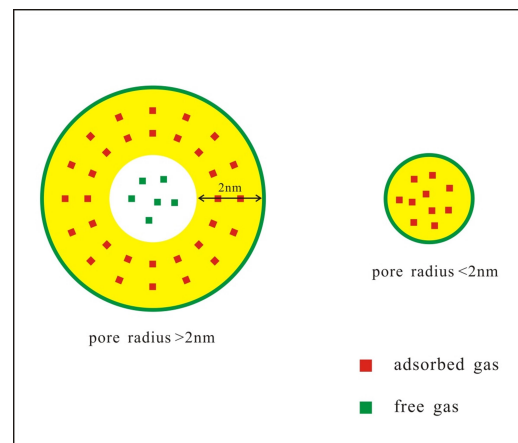


Fig. 10. Occurrence state of shale gas in pores of different size.

- 1) The Lower Silurian shale in the Upper Yangtze Platform contain high TOC content ranging from 0.92% to 4.96%, high quartz content in the range of 30.6%-69.5%, and high clays content ranging from 24.1% to 51.2%. The TOC content shows a strong positive relationship with the quartz content which suggests that the quartz is mainly biogenic in origin.
- 2) The micropore volume varies from 0.12 to 0.44  $\text{cm}^3/100\text{g}$  and micropore surface area varies from 4.97 to 17.94  $\text{m}^2/\text{g}$ . Both of them increase with increasing TOC content, indicating TOC is the key factor to control the micropore structure of the Lower Silurian shale.
- 3) Low pressure  $\text{CO}_2$  adsorption measurement provides the most suitable detection range (0.3-1.5 nm) and has high reliability and accuracy for micropore structure characterization.
- 4) The TOC content is the key factor to control gas adsorption capacity of the Lower Silurian shale in the Upper Yangtze Platform and attributed this to increasing micropore surface area with increasing TOC content.

Other micropore characterization techniques such as focused ion beam-Helium ion microscopy (FIB-HIM), ultra-low pressure  $\text{N}_2$  adsorption, small-angle and ultra-small-angle neutron scattering (SANS and USANS) need to be further studied to characterize the micropore structure of Lower Silurian shale. Meanwhile, high-pressure methane sorption measurements need to be performed to provide a better understanding between micropore structure and shale gas adsorption capacity.

## Acknowledgements

The authors would like to acknowledge the financial support of the National Science and Technology Major Project (No. 2016ZX05034-001) and National Natural Science Foundation of China (No. 41472112).

**Open Access** This article is distributed under the terms and conditions of the Creative Commons Attribution (CC BY-NC-ND) license (<http://creativecommons.org/licenses/by-nc-nd/4.0/>), which permits unrestricted use, distribution, and reproduction in any medium, provided the original work is properly cited.

## References

- Bu, H.L., Ju, Y.W., Tan, J.Q., et al. Fractal characteristics of pores in non-marine shales from the Huainan coalfield, eastern China. *J. Nat. Gas Sci. Eng.* 2015, 24: 166-177.
- Cai, Z.R., Huang, Q.T., Xia, B., et al. Differences in shale gas exploration prospects of the upper Yangtze Platform and the lower Yangtze Platform: Insights from computer modelling of tectonic development. *J. Nat. Gas Sci. Eng.* 2016, 36: 42-53.
- Cao, T.T., Song, Z.G., Wang, S.B., et al. Characterizing the pore structure in the Silurian and Permian shales of the Sichuan Basin, China. *Mar. Pet. Geol.* 2015, 61: 140-150.
- Chalmers, G.R.L., Bustin, R.M. Lower Cretaceous gas shales in northeastern British Columbia, Part I: geological controls on methane sorption capacity. *Bull. Can. Pet. Geol.* 2008, 56: 1-21.
- Chalmers, G.R.L., Bustin, R.M., Power, I.M. Characterization of gas shale pore systems by porosimetry, pycnometry, surface area, and field emission scanning electron microscopy/transmission electron microscopy image analyses: Examples from the Barnett, Woodford, Haynesville, Marcellus, and Doig units. *AAPG Bull.* 2012, 96: 1099-1119.
- Chen, J., Xiao, X.M. Evolution of nanoporosity in organic-rich shales during thermal maturation. *Fuel* 2014, 129: 173-181.
- Chen, L., Jiang, Z.X., Liu, K.Y., et al. Effect of lithofacies on gas storage capacity of marine and continental shales in the Sichuan Basin, China. *J. Nat. Gas Sci. Eng.* 2016, 36: 773-785.
- Chen, L., Jiang, Z.X., Liu, K.Y., et al. Application of Langmuir and Dubinin-Radushkevich models to estimate methane sorption capacity on two shale samples from the Upper Triassic Chang 7 Member in the southeastern Ordos Basin, China. *Energy Explor. Exploit.* 2017a, 35(1): 122-144.
- Chen, L., Jiang, Z.X., Liu, K.Y., et al. Pore structure characterization for organic-rich Lower Silurian shale in the Upper Yangtze Platform, South China: A possible mechanism for pore development. *J. Nat. Gas Sci. Eng.* 2017b, 46: 1-15.
- Chen, S.B., Zhu, Y.M., Qin, Y., et al. Reservoir evaluation of the Lower Silurian Longmaxi Formation shale gas in the southern Sichuan Basin of China. *Mar. Pet. Geol.* 2014, 57: 619-630.
- Chen, S.B., Zhu, Y.M., Wang, H.Y., et al. Shale gas reservoir characterisation: A typical case in the southern Sichuan Basin of China. *Energy* 2011, 36: 6609-6616.
- Clarkson, C.R., Solano, N., Bustin, R.M., et al. Pore structure characterization of North American shale gas reservoirs using USANS/SANS, gas adsorption, and mercury intrusion. *Fuel* 2013, 103: 606-616.
- Curtis, M.E., Sondergeld, C.H., Ambrose, R.J., et al. Microstructural investigation of gas shales in two and three dimensions using nanometer-scale resolution imaging. *AAPG Bull.* 2012, 96: 665-677.
- Dong, T., Harris, N.B., Ayranci, K., et al. Porosity characteristics of the Devonian Horn River shale, Canada: Insights from lithofacies classification and shale composition. *Int. J. Coal Geol.* 2015, 141: 74-90.
- Du, X.B., Song, X.D., Zhang, M.Q., et al. Shale gas potential of the Lower Permian Gufeng Formation in the western area of the Lower Yangtze Platform, China. *Mar. Pet. Geol.* 2015, 67: 526-543.
- Dubinina, M.M. Generalization of the theory of volume filling of micropores to nonhomogeneous microporous structures. *Carbon* 1985, 23: 373-380.
- Gasparik, M., Bertier, P., Gensterblum, Y., et al. Geological controls on the methane storage capacity in organic-rich shales. *Int. J. Coal Geol.* 2014, 123: 34-51.
- Giesche, H. Mercury porosimetry: A general (practical) overview. *Part. Part. Syst. Character.* 2006, 23: 9-19.
- Gu, X., Cole, D.R., Rother, G., et al. Pores in Marcellus shale: A neutron scattering and FIB-SEM study. *Energy Fuels* 2015, 29: 1295-1308.
- Hao, F., Zou, H.Y., Lu, Y.C. Mechanisms of shale gas storage: Implications for shale gas exploration in China. *AAPG Bull.* 2013, 97: 1325-1346.
- Hu, H.Y., Zhang, T.W., Wiggins-Camacho, J.D., et al. Experimental investigation of changes in methane adsorption of bitumen-free Woodford Shale with thermal maturation induced by hydrous pyrolysis. *Mar. Pet. Geol.* 2015, 59: 114-128.
- Ji, W.M., Song, Y., Jiang, Z.X., et al. Estimation of marine shale methane adsorption capacity based on experimental investigations of Lower Silurian Longmaxi formation in the Upper Yangtze Platform, south China. *Mar. Pet. Geol.* 2015, 68: 94-106.
- Ji, W.M., Song, Y., Jiang, Z.X., et al. Fractal characteristics of nano-pores in the Lower Silurian Longmaxi shales from the Upper Yangtze Platform, south China. *Mar. Pet. Geol.* 2016, 78: 88-98.
- Jiang, S., Peng, Y.M., Gao, B., et al. Geology and shale gas resource potentials in the Sichuan Basin, China. *Energy Explor. Exploit.* 2016, 34(5): 689-710.
- Jiao, K., Yao, S.P., Liu, C., et al. The characterization and quantitative analysis of nanopores in unconventional gas reservoirs utilizing FESEM-FIB and image processing: An example from the lower Silurian Longmaxi Shale, upper Yangtze region, China. *Int. J. Coal Geol.* 2014, 128: 1-11.
- Jing, T.Y., Zhang, J.C., Xu, S.S., et al. Critical geological characteristics and gas-bearing controlling factors in Longmaxi shales in southeastern Chongqing, China. *Energy Explor. Exploit.* 2016, 34(1): 42-60.
- Klaver, J., Desbois, G., Littke, R., et al. BIB-SEM characterization of pore space morphology and distribution in postmature to overmature samples from the Haynesville and Bossier Shales. *Mar. Pet. Geol.* 2015, 59: 451-466.
- Klaver, J., Desbois, G., Littke, R., et al. BIB-SEM pore characterization of mature and post mature Posidonia Shale samples from the Hils area, Germany. *Int. J. Coal Geol.* 2016, 158: 78-89.
- Li, J.J., Yan, X.T., Wang, W.M., et al. Key factors controlling the gas adsorption capacity of shale: A study based on

- parallel experiments. *Appl. Geochem.* 2015a, 58: 88-96.
- Li, J.J., Yin, J.X., Zhang, Y.N., et al. A comparison of experimental methods for describing shale pore features: A case study in the Bohai Bay Basin of eastern China. *Int. J. Coal Geol.* 2015b, 152: 39-49.
- Li, J., Zhou, S.X., Li, Y.J., et al. Effect of organic matter on pore structure of mature lacustrine organic-rich shale: A case study of the Triassic Yanchang shale, Ordos Basin, China. *Fuel* 2016, 185: 421-431.
- Li, Z.Q., Oyediran, I.A., Huang, R.Q., et al. Study on pore structure characteristics of marine and continental shale in China. *J. Nat. Gas Sci. Eng.* 2016, 33: 143-152.
- Liu, J., Yao, Y.B., Zhu, Z.J., et al. Experimental investigation of reservoir characteristics of the upper Ordovician Wufeng Formation shale in middle-upper Yangtze region, China. *Energy Explor. Exploit.* 2016, 34(4): 527-542.
- Loucks, R.G., Reed, R.M., Ruppel, S.C., et al. Spectrum of pore types and networks in mudrocks and a descriptive classification for matrix-related mudrock pores. *AAPG Bull.* 2012, 96: 1071-1098.
- Mastalerz, M., He, L.L., Melnichenko, Y.B., et al. Porosity of coal and shale: Insights from gas adsorption and SANS/USANS techniques. *Energy Fuels* 2012, 26: 5109-5120.
- Mastalerz, M., Schimmelmann, A., Drobniak, A., et al. Porosity of Devonian and Mississippian New Albany Shale across a maturation gradient: Insights from organic petrology, gas adsorption, and mercury intrusion. *AAPG Bull.* 2013, 97: 1621-1643.
- Milliken, K.L., Rudnicki, M., Awwiller, D.N., et al. Organic matter-hosted pore system, Marcellus Formation (Devonian), Pennsylvania. *AAPG Bull.* 2013, 97: 177-200.
- Mosher, K., He, J.J., Liu, Y.Y., et al. Molecular simulation of methane adsorption in micro- and mesoporous carbons with applications to coal and gas shale systems. *Int. J. Coal Geol.* 2013, 109: 36-44.
- Pan, L., Xiao, X.M., Tian, H., et al. A preliminary study on the characterization and controlling factors of porosity and pore structure of the Permian shales in Lower Yangtze region, Eastern China. *Int. J. Coal Geol.* 2015, 146: 68-78.
- Pan, L., Xiao, X.M., Tian, H., et al. Geological models of gas in place of the Longmaxi shale in Southeast Chongqing, South China. *Mar. Pet. Geol.* 2016, 73: 433-444.
- Rexer, T.F.T., Benham, M.J., Aplin, A.C., et al. Methane adsorption on shale under simulated geological temperature and pressure conditions. *Energy Fuels* 2013, 27: 3099-3109.
- Romero-Sarmiento, M.F., Rouzaud, J.N., Bernard, S., et al. Evolution of Barnett Shale organic carbon structure and nanostructure with increasing maturation. *Org. Geochem.* 2014, 71: 7-16.
- Ross, D.J.K., Bustin, R.M. The importance of shale composition and pore structure upon gas storage potential of shale gas reservoirs. *Mar. Pet. Geol.* 2009, 26: 916-927.
- Sing, K.S.W. Reporting physisorption data for gas/solid systems with special reference to the determination of surface area and porosity (Recommendations 1984). *Pure Appl. Chem.* 1985, 57: 603-619.
- Slatt, R.M., O'Brien, N.R. Pore types in the Barnett and Woodford gas shales: Contribution to understanding gas storage and migration pathways in fine-grained rocks. *AAPG Bull.* 2011, 95: 2017-2030.
- Stoekli, F., Ballerini, L. Evolution of microporosity during activation of carbon. *Fuel* 1991, 70: 557-559.
- Sun, M.D., Yu, B.S., Hu, Q.H., et al. Nanoscale pore characteristics of the Lower Cambrian Niutitang Formation Shale: A case study from Well Yuke #1 in the Southeast of Chongqing, China. *Int. J. Coal Geol.* 2016, 154: 16-29.
- Tan, J.Q., Weniger, P., Krooss, B., et al. Shale gas potential of the major marine shale formations in the Upper Yangtze Platform, South China, Part II: Methane sorption capacity. *Fuel* 2014, 129: 204-218.
- Tang, X.L., Jiang, Z.X., Jiang, S., et al. Heterogeneous nanoporosity of the Silurian Longmaxi Formation shale gas reservoir in the Sichuan Basin using the QEMSCAN, FIB-SEM, and nano-CT methods. *Mar. Pet. Geol.* 2016, 78: 99-109.
- Tian, H., Pan, L., Xiao, X.M., et al. A preliminary study on the pore characterization of Lower Silurian black shales in the Chuandong Thrust Fold Belt, southwestern China using low pressure N<sub>2</sub> adsorption and FE-SEM methods. *Mar. Pet. Geol.* 2013, 48: 8-19.
- Tian, H., Pan, L., Zhang, T.W., et al. Pore characterization of organic-rich Lower Cambrian shales in Qiannan Depression of Guizhou Province, Southwestern China. *Mar. Pet. Geol.* 2015, 62: 28-43.
- Wang, S.B., Song, Z.G., Cao, T.T., et al. The methane sorption capacity of Paleozoic shales from the Sichuan Basin, China. *Mar. Pet. Geol.* 2013, 44: 112-119.
- Wei, L., Mastalerz, M., Schimmelmann, A., et al. Influence of Soxhlet-extractable bitumen and oil on porosity in thermally maturing organic-rich shales. *Int. J. Coal Geol.* 2014, 132: 38-50.
- Wei, M.M., Xiong, Y.Q., Zhang, L., et al. The effect of sample particle size on the determination of pore structure parameters in shales. *Int. J. Coal Geol.* 2016a, 163: 177-185.
- Wei, M.M., Zhang, L., Xiong, Y.Q., et al. Nanopore structure characterization for organic-rich shale using the non-local-density functional theory by a combination of N<sub>2</sub> and CO<sub>2</sub> adsorption. *Microporous Mesoporous Mater.* 2016b, 227: 88-94.
- Wu, Y., Fan, T.L., Jiang, S., et al. Methane adsorption capacities of the lower paleozoic marine shales in the Yangtze Platform, South China. *Energy Fuels* 2015, 29: 4160-4167.
- Yang, F., Ning, Z.F., Wang, Q., et al. Pore structure characteristics of lower Silurian shales in the southern Sichuan Basin, China: Insights to pore development and gas storage mechanism. *Int. J. Coal Geol.* 2016a, 156: 12-24.
- Yang, F., Ning, Z.F., Wang, Q., et al. Pore structure of Cambrian shales from the Sichuan Basin in China and implications to gas storage. *Mar. Pet. Geol.* 2016b, 70: 14-26.

- Yang, R., He, S., Hu, Q.H., et al. Pore characterization and methane sorption capacity of over-mature organic-rich Wufeng and Longmaxi shales in the southeast Sichuan Basin, China. *Mar. Pet. Geol.* 2016c, 77: 247-261.
- Zeng, J., Jia, W.L., Peng, P.A., et al. Composition and pore characteristics of black shales from the Ediacaran Lantian Formation in the Yangtze Block, South China. *Mar. Pet. Geol.* 2016, 76: 246-261.
- Zhang, T.W., Ellis, G.S., Ruppel, S.C., et al. Effect of organic-matter type and thermal maturity on methane adsorption in shale-gas systems. *Org. Geochem.* 2012, 47: 120-131.
- Zhang, X., Liu, C.L., Zhu, Y.M., et al. The characterization of a marine shale gas reservoir in the lower Silurian Longmaxi Formation of the northeastern Yunnan Province, China. *J. Nat. Gas Sci. Eng.* 2015, 27: 321-335.
- Zhou, S.W., Yan, G., Xue, H.Q., et al. 2D and 3D nanopore characterization of gas shale in Longmaxi formation based on FIB-SEM. *Mar. Pet. Geol.* 2016, 73: 174-180.